*Int. J. Electrochem. Sci.*, 12 **(2017)** 155 – 165, doi: 10.20964/2017.01.62

International Journal of
ELECTROCHEMICAL
SCIENCE
www.electrochemsci.org

# Microstructure and Corrosion Resistance Studies of PEO Coated Mg Alloys with a HF and US Pretreatment

*Fangfang Wei*[1,2], *Wei Zhang*[2,*], *Tao Zhang*[2,*], *Fuhui Wang*[2]

[1] School of Materials Science and Engineering, University of Science and Technology of China, Hefei, 230026, China
[2] Laboratory for Corrosion and Protection, Institute of Metal Research, Chinese Academy of Sciences, No. 62 Wencui Road, Shenyang, 110016, China
[*]E-mail: ffwei12b@imr.ac.cn

*Received:* 3 November 2016 / *Accepted:* 6 December 2016 / *Published:* 12 December 2016

The effect of hydrofluoric acid (HF) pretreatment on the microstructure and corrosion resistance of PEO coatings on AZ91 Mg alloys was investigated. The results showed that thin fluoride film was formed on AZ91 Mg alloy after pretreatment. The application of ultrasound (US) in the pretreatment made the film more compact and increased its F content. PEO coatings deposited on the pretreated AZ91 become denser with decreased porosity level and have no structural defects. The inner layer (IL) of PEO coating of HF-treated AZ91 with US is more intact and contains more F than those obtained without US. The better quality of IL could facilitate the stable discharge and form compact PEO coating. Therefore, PEO coating deposited on AZ91 pretreated with (HF+US) offered a better corrosion resistance, which is in good agreement with the results of electrochemical measurements.

**Keywords:** Mg alloys; Plasma electrolytic oxidation; Oxide coatings; pretreatment; corrosion

## 1. INTRODUCTION

Plasma electrolytic oxidation (PEO) is an effective surface modification technique, which produces a hard, well adherent, moderate corrosion resistance ceramic oxide coating on the surface of valve metals [1, 2]. Therefore, PEO method is widely used to improve the corrosion resistance of metals, especially Al, Mg [3-6]. The PEO coatings grow above the dielectric breakdown voltage at the sites of plasma discharge, where pores act as channels caused by plasma discharge could influence the corrosion resistance of PEO coatings [7-10].

Several strategies [11] were explored to improve the corrosion resistance of PEO coatings of Mg alloys in recent years, including choice of the electrolytes [12,13], optimize process parameters and conditions [14,15], additives and incorporation of ceramic particles [16-19], sealing [20] and post

treatment [21,22], and pretreatment on substrate. The constituents of the PEO coating which have great effect on the corrosion resistance originate from the substrate and the electrolyte. Therefore, without changing the electrolyte, combining the pretreatment of substrate, the PEO coating may be incorporated into special element and its corrosion resistance could be improved. Up to now, few researchers focus on the pretreatment [23,24] on substrate for improving the corrosion resistance of PEO coatings of Mg alloys. It was reported that the corrosion resistance of PEO coating with pretreatment using cerium conversion coating offered a better corrosion resistance, which is attributed to high P-B ratio and insulativity of rare earth oxides existence in PEO coating [23]. It was investigated the use of laser surface melting (LSM) as a pretreatment and obtained better corrosion resistance, which is due to the higher content of $MgAl_2O_4$ in the coating and more compact cross-sectional structure [24]. However, above methods increase the complexity and the cost of the technical process.

HF treatment [25] has been studied as an acid pickling treatment of Mg alloys, an undissolved $MgF_2$ film could be generated on the surface during the treatment, which makes it possible to avoid the excessive anodic dissolution of the Mg alloy. Moreover, if $MgF_2$ can be synthesized into the PEO coating and replace the MgO as the main phase, which would reduce the porosity level of coating.

In this paper, HF with or without US treatment was for the first time proposed as a pretreatment taken on AZ91 which can alter the microstructure of PEO coating aimed to improve the corrosion resistance of AZ91.

## 2. EXPERIMENTAL

### *2.1 Pretreatment processing*

As-cast AZ91 Mg alloys (Al 8.96, Zn 0.64, Mn 0.16, Si 0.015, Cu<0.005, Fe 0.012, Ni<0.005, Mg Balance, wt.%) with dimensions of 30 mm × 35 mm × 8 mm were employed and ground with emery paper up to 1000#, rinsed with ethanol and deionized water, then dried by cool air. In this paper, the specimen with this treatment was called “AZ91”. Before PEO process, AZ91 Mg alloys samples were pretreated by dipping in HF (9.8 wt.%) for 30 s (25 ± 1°C) with and without US, the specimens with this two methods were called “AZ91+HF” and “AZ91+HF+US”, respectively. Then flushed by deionized water and dried by cool air. The US was applied with a constant frequency of 40 kHz and a constant power of 60 W.

### *2.2 PEO process*

Three kinds of the specimens with different pretreatment methods which called as “AZ91”, “AZ91+HF” and “AZ91+HF+US” were treated by PEO. The specimen and a graphite plate were used as the anode and the cathode, respectively. The electrolytes were composed of 15 g/L $Na_2SiO_3 \cdot 9H_2O$, 5 g/L $KF \cdot 2H_2O$ and 2 g/L NaOH. The PEO process was performed with a 50 kW pulsed direct-current

power source. The technic parameters including frequency, constant current density, duty cycle and oxidation time were fixed at 1 KHz, 0.02 A/cm$^2$, 10 min, 50% and 30 min, respectively.

### *2.3 Microstructure characterization*

The microstructure of sample was characterized by scanning electron microscopy (SEM) attached with an X-ray energy dispersive spectrometer (EDS) system, which was further investigated by transmission electron microscopy (TEM) attached with an EDS system. The methods for thin foils preparation can be found in our previous study [26].

### *2.4 Electrochemical measurement*

The potentiodynamic polarization was performed using the Zahner Zennium electrochemical workstation and a three-electrode cell system. A saturated calomel electrode (SCE) was used as the reference electrode and a platinum plate as the counter electrode. The specimen was used as working electrode (WE) and the area was 1 cm$^2$ exposed to 3.5 wt.% NaCl solution. Potential scanning was conducted at a rate of 0.5 mV/s after 10 min of immersion. The corrosion potential ($E_{corr}$) and corrosion current density ($i_{corr}$) were determined by Tafel extrapolation method from the potentiodynamic polarization curves.

Electrochemical noise (EN) measurements were performed within a Faraday cage with an Autolab electrochemical workstation equipped with EN module. Two identical specimens were used as the WE and a SCE as the reference electrode. The electrochemical current noise was measured as the galvanic coupling current between two identical WE kept at the same potential. Each set of EN records, containing 14400 data points, recorded with a data-sampling interval of 0.25 s. The noise data were collected for 432,000 s immersion period.

For better reproducibility, all of the electrochemical measurements were repeated at least three times. Temperature was maintained at 25 ± 1℃.

## 3. RESULTS AND DISCUSSION

### *3.1 The effect of pretreatment on the voltage behavior of PEO process*

Fig. 1. shows the voltage-time curves of PEO treated AZ91. Three stages can be identified according to discharge characteristics [2].

It is clear that the breakdown voltage of AZ91, AZ91+HF and AZ91+HF+US were measured to be from 266 V fell to 257 V and 242 V, and the final voltages were found to be 448±2, 445±3, and 437±3 V, respectively. The lower breakdown voltage could be attributed to the introduction of fluoride into PEO coating during the pretreatment process which is likely to be incorporated in the passive oxide coating, which can promote arcing over the whole surface in PEO process, consequently the sparking voltage could be easily reached. The different final voltage could be explained from that the

density of plasma discharge decreased due to the enhancement of thickness and compactness of the coatings. The stage Ⅱ of AZ91+HF+US was the longest samples, which demonstrated that the formed PEO coatings of AZ91+HF+US is more uniform and compact. The results were consistent with the previous study [27].

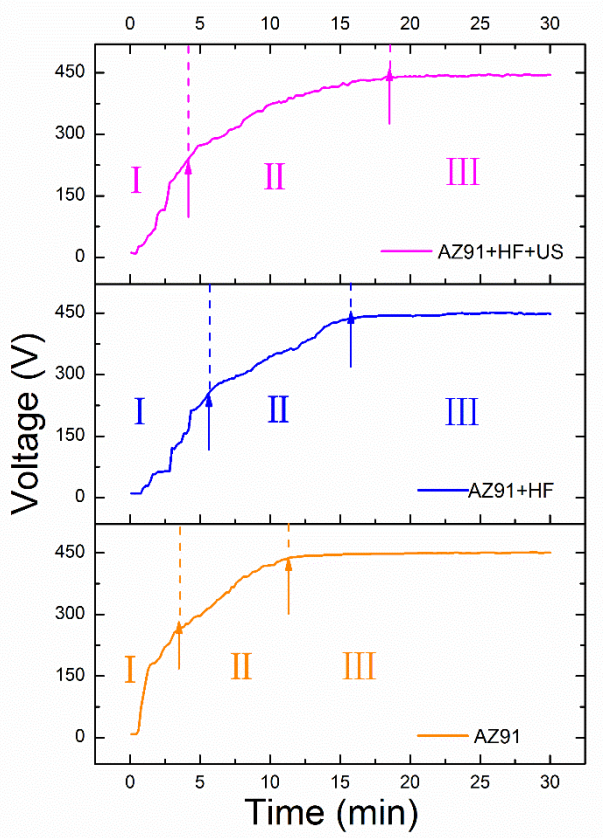


**Figure 1.** Voltage-time curves of PEO process performed on AZ91 Mg alloys pretreated with different methods for 30 min at 2 A/dm$^2$ in alkaline electrolyte containing 15 g/L $Na_2SiO_3 \cdot 9H_2O$, 5 g/L $KF \cdot 2H_2O$ and 2 g/L NaOH at 298 K

### *3.2 The effect of pretreatment on the microstructure and composition of Mg alloys and theirs PEO coatings*

The grooves exhibited between the interfaces of β-$Mg_{17}Al_{12}$/(α+β)/α phase in pretreated AZ91 (Fig. 2b and 2c) as compared to none pretreated AZ91 (Fig. 2a). From EDS results, it can be seen that F content increased and Al content decreased after pretreatment, indicating that α-Mg passivated rapidly and β phase dissolved preferentially in HF. The application of US enhanced the dissolution of β phase due to the cavitation damage of US [28]. Furthermore, US resulted in the increase of F content in the PEO coating. In addition, a thin film was observed on the cross-section images of pretreated AZ91 (Fig. 2d-2e) and further characterized by TEM (Fig. 2f-2g). The selected area electron diffraction (SAED) pattern of which consisted of diffraction rings represented $MgF_2$, MgO and $AlF_3$. From the STEM-EDS mapping images, it can be concluded that F distributed uniformly in AZ91+HF+US, and the fluoride film is more compact than AZ91+HF.

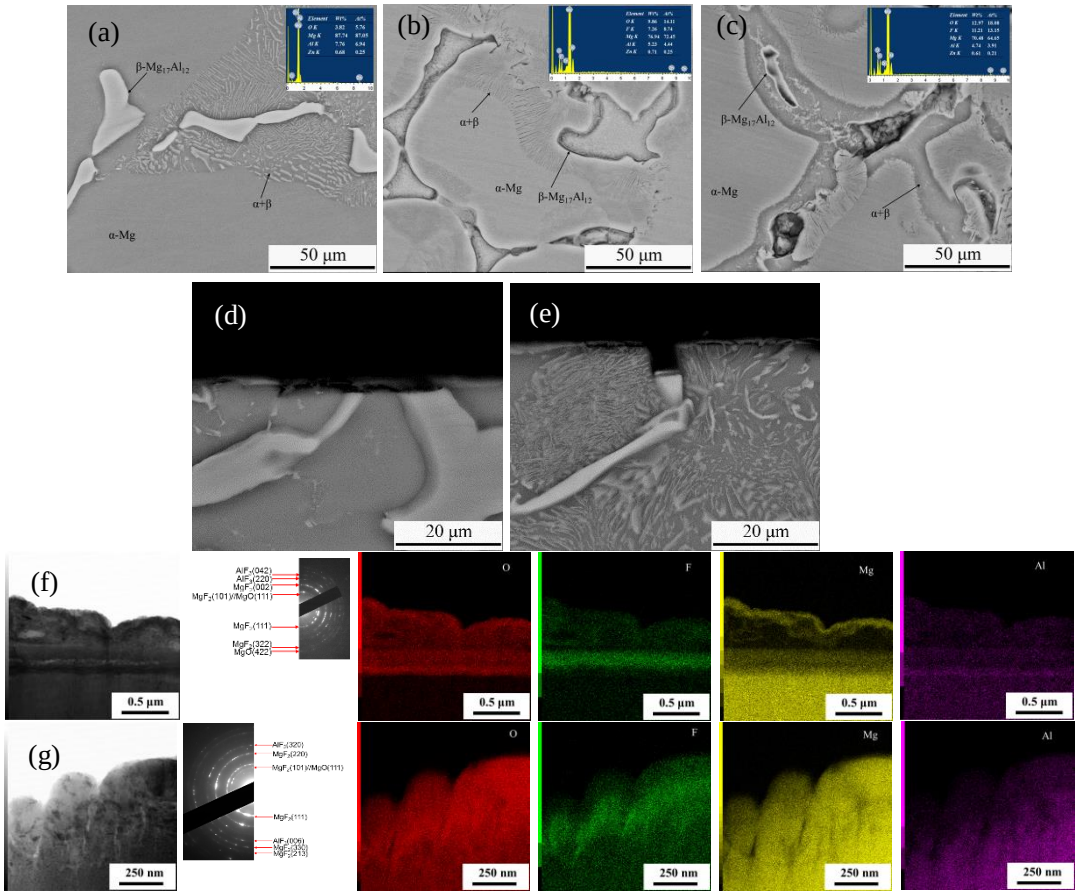


**Figure 2.** The surface and cross-sectional morphologies of AZ91 Mg alloys pretreated with different methods (a) AZ91 (b)(d) AZ91+HF (c)(e) AZ91+HF+US (Insets) EDS results. Cross-section TEM images, SAED patterns and STEM-mapping of AZ91 Mg alloys (f) pretreated in HF (g) pretreated in HF with US

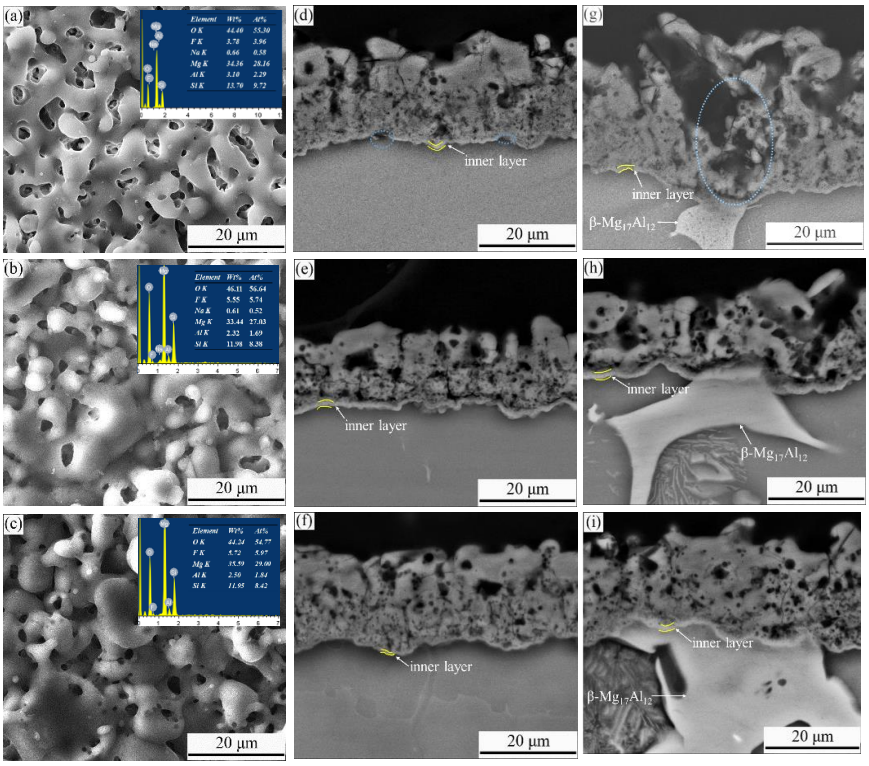

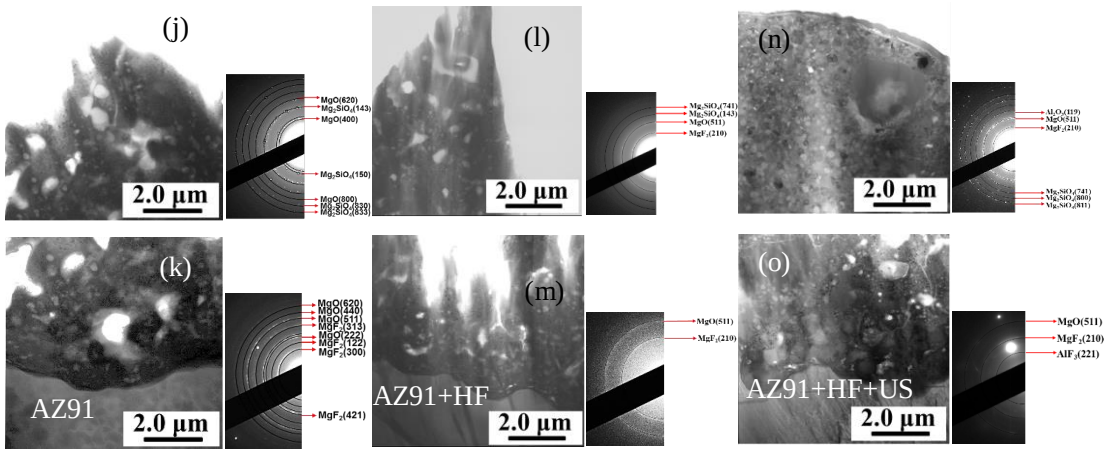


**Figure 3.** The surface and cross-sectional morphologies of PEO coatings of (a)(d)(g) AZ91 (b)(e)(h) AZ91+HF (c)(f)(i) AZ91+HF+US, respectively. (Insets) EDS results. Cross-section TEM images, SAED patterns and Element mapping of PEO coated AZ91 Mg alloys (j)(l)(n) the outer layer (OL) and SAED patterns taken from corresponding region (k)(m)(o) the IL near coating/substrate interface and SAED patterns taken from corresponding region

These results indicated that AZ91+HF+US were covered with homogeneous fluoride layer, in metallographic and electrochemical terms, which eliminated the difference between the different phases and made the surface of AZ91 have homogeneous activity.

Fig. 3a-3i displays the surface and cross-section morphologies of the PEO coatings of AZ91, as well as the EDS results. The EDS results show that F content increased after HF pretreatment, indicating that fluoride film became incorporated into the PEO coating.

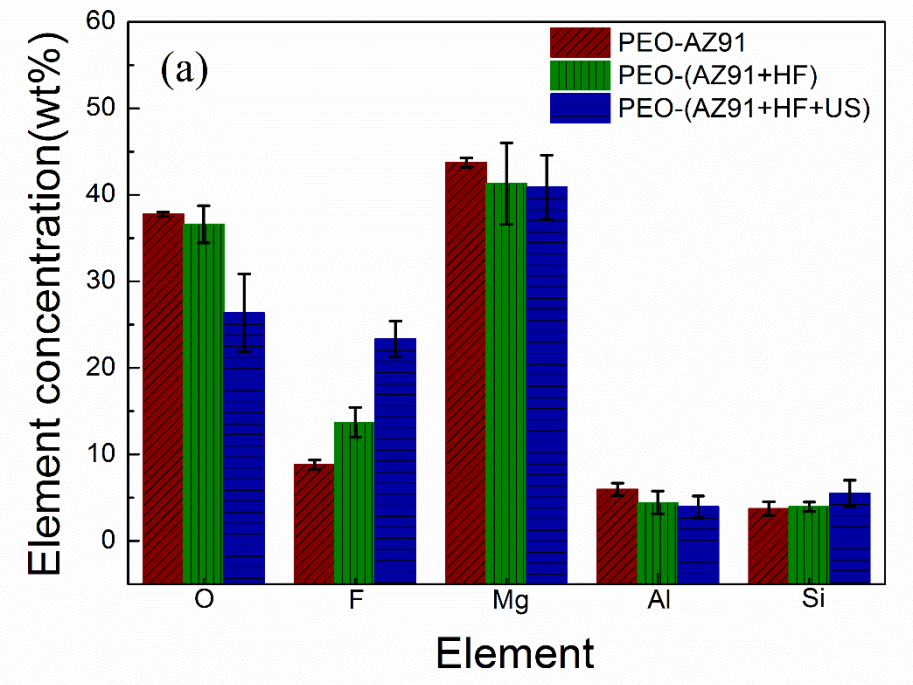

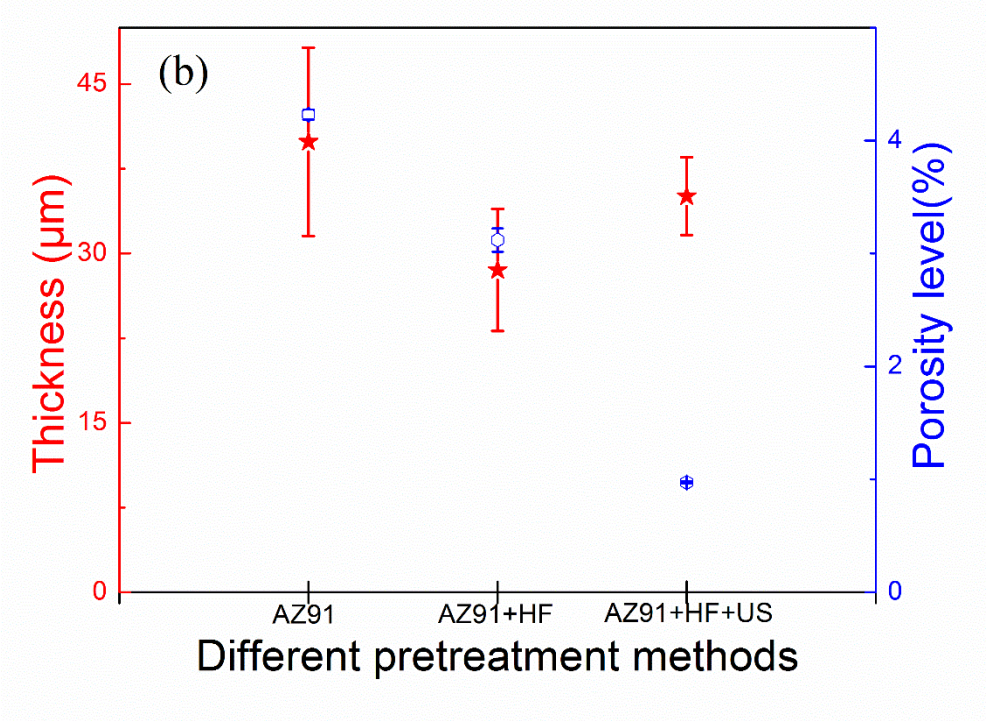


**Figure 4.** (a) Distribution of the main elements measured by EDS analysis on cross sections from the IL of PEO coatings of AZ91, AZ91+HF and AZ91+HF+US. (b) Thickness and porosity level of PEO coatings deposited on AZ91, AZ91+HF and AZ91+HF+US

The IL of PEO coatings of AZ91 was incomplete and have structural defects in β phase (marked by the blue dashed line in Fig. 3d-3g), which is attributed to B-type discharge which could extend to the coating-substrate interface [29, 30]. The IL of PEO coatings of (AZ91+HF) and (AZ91+HF+US) is intact and free-defects. It could be concluded that HF pretreatment have beneficial effect on the quality of PEO coatings.

The detailed microstructure of PEO coatings was further characterized by TEM (Fig. 3j-3o), which was consistent with SEM results. Moreover, the nanocrystalline of $Al_2O_3$ was verified by SAED pattern in PEO coatings of (AZ91+HF+US). Further research in the future, however, is important to provide more understanding about the formation of $Al_2O_3$.

The microstructural evolution including the element content, porosity level and average coating thickness of PEO coatings were presented in Fig. 4a and 4b.

It can be found that F content increased significantly in IL after AZ91 pretreated in HF, especially with application of US. The greater the proportion of the fluoride in IL, the more stable of the discharge in PEO process [31,32], which bring the good quality of PEO coatings. Therefore, the compact and intact IL may be responsible for the lower porosity level of coating. Moreover, the better quality of IL could facilitate the production of localized discharge on AZ91 [8], which contribute to the coating growth. The coating thickness of PEO-AZ91 is the thickest, but very uneven, which could be concluded from the error and caused by unstable discharge in PEO process. The coating thickness of PEO-(AZ91+HF+US) is second only to PEO-AZ91, but displays less error, which on behalf of the uniformity of coating.

### *3.3 Electrochemical corrosion behavior of different PEO coatings*

#### *3.3.1 Potentiodynamic polarization*

The potentiodynamic polarization curves of the PEO coatings on different pretreated AZ91 were shown in Fig. 5. The corresponding electrochemical data anodic and cathodic Tafel slopes ($\beta_a$ and $\beta_c$), $E_{corr}$ and $i_{corr}$ derived from the polarization curves, the polarization resistance ($R_p$) values were calculated using the relationship [33,34]:

$$R_p = \frac{\beta_a \beta_c}{2.303 i_{corr} (\beta_a + \beta_c)}$$

All the above parameters were listed in Table 1. The PEO-AZ91 had the lowest anodic Tafel slope, which was attributed to the coatings have higher porosity level than those of PEO coatings deposited on AZ91 with pretreatment. The anodic Tafel slope of PEO-(AZ91+HF+US) was higher than PEO-(AZ91+HF) due to the coating thicker in thickness and incorporated of more fluoride, which could be attributed to the application of US facilitated the formation of PEO coatings with free of structural defects. [27] Therefore, the occurrence of pitting corrosion could be delayed. The $E_{corr}$ of PEO-(AZ91+HF) and PEO-(AZ91+HF+US) towards the active potential shift and the noble potential shift as compared to that of PEO-AZ91, respectively.

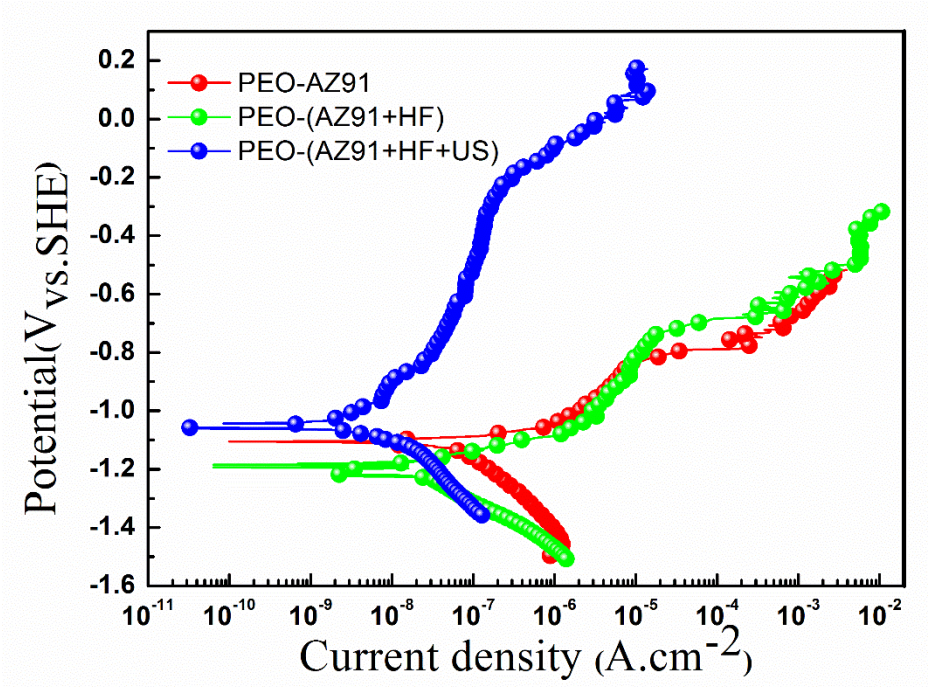


**Figure 5.** Potentiodynamic polarization curves for PEO coatings of AZ91, AZ91+HF and AZ91+HF+US in 3.5 wt.% NaCl solution.

**Table 1.** Electrochemical data of PEO coatings of AZ91 Mg alloys pretreated differently obtained by potentiodynamic polarization curves

| Specimens | $\beta_a$ | $\beta_c$ | $E_{corr}$ | $i_{corr}$ | $R_p$ |
|---|---|---|---|---|---|

| | (mV/dec) | (-mV/dec) | (V vs. SHE) | ($A/cm^2$) | ($\Omega\ cm^2$) |
|---|---|---|---|---|---|
| PEO-AZ91 | 210.26 | 221.36 | -1.106±0.002 | $(1.020\pm0.012)\times10^{-8}$ | $(4.59\pm0.039)\times10^{6}$ |
| PEO-(AZ91+HF) | 270.36 | 159.38 | -1.193±0.021 | $(1.014\pm0.065)\times10^{-8}$ | $(4.29\pm0.670)\times10^{6}$ |
| PEO-(AZ91+HF+US) | 550.97 | 300.80 | -1.053±0.005 | $(6.575\pm0.091)\times10^{-9}$ | $(1.28\pm0.928)\times10^{7}$ |

The passivation potential range for PEO-(AZ91+HF+US) was 770 mV, which was higher than PEO-(AZ91+HF) (410 mV) and PEO-AZ91 (240 mV). Moreover, the $i_{corr}$ of PEO-(AZ91+HF+US) was lower than the others, the $R_p$ of PEO-(AZ91+HF+US) was the biggest among these samples, indicating that it has a lowest corrosion rate. These findings all presented that the PEO coating formed on AZ91 pretreated in HF with US offered a best corrosion resistance. Furthermore, the $i_{corr}$ and $R_p$ of PEO coated AZ91 pretreated with HF with US was comparable to the reported values [23,24,27], implying that the HF with US pretreatment was an effective method for improving the corrosion resistance of PEO coatings of Mg alloys.

### *3.3.2 Comparison of corrosion resistance of different PEO coatings by electrochemical noise measurements*

Electrochemical noise data analysis in the time domain involves the calculation of the noise resistance ($R_n$), which is defined as the ratio of a standard deviation of the potential to that of the current noise. The results of EN measurements were shown in Fig. 6.

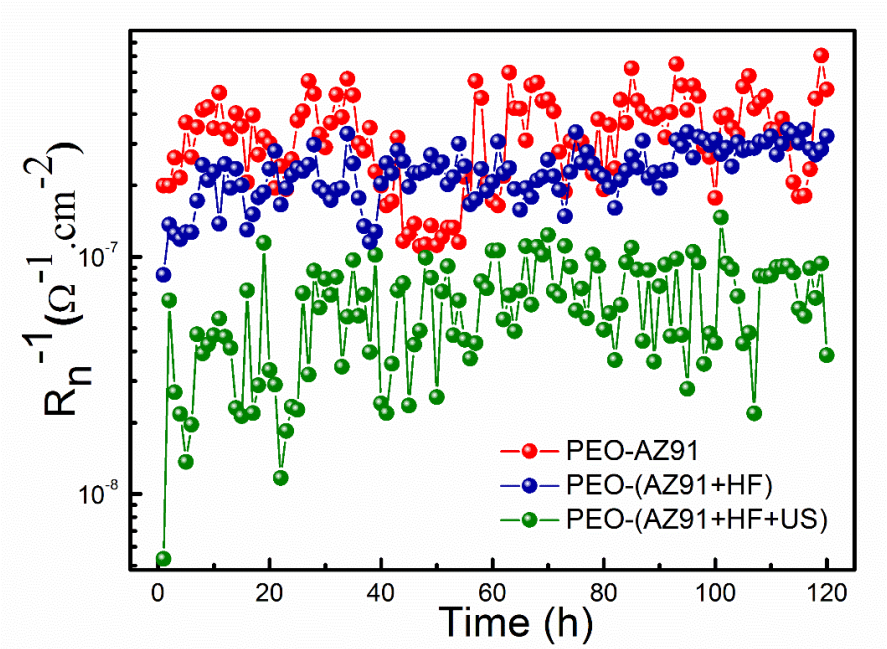


**Figure 6.** The reciprocal of $R_n$ for PEO coatings deposited on AZ91, AZ91+HF and AZ91+HF+US during a 120 h period in 3.5 wt.% NaCl solution.

During the immersion period, the values of $1/R_n$ of PEO-AZ91 was the biggest in all, which was about two times higher than that of PEO-(AZ91+HF), seven times higher than that of PEO-(AZ91+HF+US). It is well known $R_n$ varied inversely with the corrosion rate [26,35,36,37], therefore, the PEO-(AZ91+HF+US) had the lowest corrosion rate. This means that PEO-(AZ91+HF+US) had the best pitting corrosion resistance than those of PEO-(AZ91+HF) and PEO-AZ91. And consequently, a similar tendency in corrosion resistance as obtained from the potentiodynamic polarization curves and as the following order: PEO-(AZ91+HF+US) > PEO-(AZ91+HF) > PEO-AZ91.

## 4. CONCLUSION

A new simple and effective pretreatment methods combining with PEO technique was proposed. The PEO coating deposited on pretreated AZ91 consisted of more fluoride and intact IL, which promoted stable spark discharge in PEO process, accordingly influence the components, thickness and porosity level of PEO coatings. The corrosion resistance of the PEO coating formed on AZ91 with pretreatment is better than the PEO coating directly formed on bare AZ91, which is verified by the electrochemical results.

ACKNOWLEDGEMENTS
The research is supported by the Key Project of Natural Science Foundation of China(NO. 51531007).

## References

1. J. A. Curran and T. W. Clyne, *Acta Mater.*, 54 (2006) 1985.
2. R. O. Hussein, X. Nie and D. O. Northwood, *Electrochim. Acta*, 112 (2013) 111.
3. R. Arrabal, E. Matykina, F. Viejo, P. Skeldon and G. E. Thompson, *Corros. Sci.*, 50 (2008) 1744.
4. P. Bala Srinivasan, C. Blawert and W. Dietzel, *Corros. Sci.*, 50 (2008) 2415.
5. W. Zhang, B. Tian, K. Du, H. Zhang and F. Wang, *Int. J. Electrochem. Sci.*, 6 (2011) 5228.
6. H. Nasiri Vatan, R. Ebrahimi-Kahrizsangi and M. Kasiri Asgarani, *Int. J. Electrochem. Sci.*, 11 (2016) 929.
7. T. B. Van, S. D. Brown and G. P. Wirtz, *Am. Ceram. Soc. Bull.*, 6 (1977) 563.
8. A. L. Yerokhin, X. Nie, A. Leyland, A. Matthews and S. J. Dowey, *Surf. Coat. Technol.*, 122 (1999) 73.
9. G. Lv, H. Chen, L. Li, E. Niu, H. Pang, B. Zou and S. Yang, *Curr. Appl. Phys.*, 9 (2009) 126.
10. L. D. Liu, S. F. Hsieh, C. Y. Lee and C. S. Lin, *J. Electrochem. Soc.*, 155 (2008) C307.
11. T. S. N. Sankara Narayanan, I. S. Park and M. H. Lee, *Prog. Mater Sci.*, 60 (2014) 1.
12. J. Liang, B. Guo, J. Tian, H. Liu, J. Zhou and T. Xu, *Appl. Surf. Sci.*, 252 (2005) 345.
13. C. Blawert, V. Heitmann, W. Dietzel, H. M. Nykyforchyn and M. D. Klapkiv, *Surf. Coat. Technol.*, 201 (2007) 8709.
14. P. Bala Srinivasan, J. Liang, R. G. Balajeee, C. Blawert, M. Störmer and W. Dietzel, *Appl. Surf. Sci.*, 256 (2010) 3928.
15. I. J. Hwang, D. Y. Hwang, Y. G. Ko and D. H. Shin, *Surf. Coat. Technol.*, 206 (2012) 3360.
16. D. Sreekanth, N. Rameshbabu and K. Venkateswarlu, *Ceram. Int.*, 38 (2012) 4607.
17. C. -E. Barchiche, E. Rocca and J. Hazan, *Surf. Coat. Technol.*, 202 (2008) 4145.
18. R. Arrabal, E. Matykina, F. Viejo, P. Skeldon, G. E. Thompson and M. C. Merino, *Appl. Surf. Sci.*,

254 (2008) 6937.
19. X. Li and B. L. Luan, *Mater. Lett.*, 86 (2012) 88.
20. H. Duan, C. Yan and F. Wang, *Electrochim. Acta*, 52 (2007) 5002.
21. Y. G. Ko, K. M. Lee, B. U. Lee and D. H. Shin, *J. Alloys Compd.*, 509S (2011) S468.
22. H. Y. Hsiao, P. Chung and W. T. Tsai, *Corros. Sci.*, 49 (2007) 781.
23. J. Cai, F. Cao, L. Chang, J. Zheng, J. Zhang and C. Cao, *Appl. Surf. Sci.*, 257 (2011) 3804.
24. L. Wang, J. Zhou, J. Liang and J. Chen, *J. Electrochem. Soc.*, 161 (2013) C20.
25. M. H. Kang, T. S. Jang, S. W. Kim, H. S. Park, J. Song, H. E. Kim, K. H. Jung and H. D. Jung, *Mater. Sci. Eng.*, C, 62 (2016) 634.
26. F. Wei, W. Zhang, T. Zhang and F. Wang, *J. Alloys Compd.*, 690 (2017) 195.
27. X. Wang, L. Zhu, H. Liu and W. Li, *Surf. Coat. Technol.*, 202 (2008) 4210.
28. G. Cravotto, S. Tagliapietra, B. Robaldo and M. Trotta, *Ultrason. Sonochem.*, 12 (2005) 95.
29. A. L. Yerokhin, L. O. Snizhko, N. L. Gurevina, A. Leyland, A. Pilkington and A. Matthews, *J. Phys. D: Appl. Phys.*, 36 (2003) 2110.
30. R. O. Hussein, X. Nie, D. O. Northwood, A. Yerokhin and A. Matthews, *J. Phys. D: Appl. Phys.*, 43 (2010) 105.
31. L. Wang, L. Chen, Z. Yan, H. Wang and J. Peng, *J. Alloys Compd.*, 480 (2009) 469.
32. L. Wang, L. Chen, Z. Yan, H. Wang and J. Peng, *J. Alloys Compd.*, 493 (2010) 445.
33. H. Duan, C. Yan and F. Wang, *Electrochim. Acta*, 52 (2007) 3785.
34. R. O. Hussein, D. O. Northwood and X. Nie, *J. Alloys Compd.*, 541 (2012) 41.
35. A. -M. Lafront, W. Zhang, S. Jin, R. Tremblay, D. Dubé and E. Ghali, *Electrochim. Acta*, 51 (2005) 489.
36. S. Bhaduri and S. B. Bhaduri, *Ceram. Int.*, 28 (2002) 153.
37. T. Zhang, X. Liu, Y. Shao, G. Meng and F. Wang, *Corros. Sci.*, 50 (2008) 3500.